Proceedings of the
International Conference on Mechanical Engineering 2003
(ICME2003) 26- 28 December 2003, Dhaka, Bangladesh

ICME2003-KEY-04

CHARACTERISTICS OF QUENCHING HIGH TEMPERATURE SURFACE WITH IMPINGING JET

Masanori MONDE

Saga University, 1 Honjo, Saga City, 840-8502, Japan

ABSTRACT

An experimental study has been conducted to understand characteristics of transient heat transfer during quenching a hot cylindrical block with an impinging water jet. The experiment was done at atmospheric pressure for the following condition: an initial block temperature of 250 and 300 ℃, a subcooling of 5 – 80 K, a jet velocity of 3 – 15 m/s, and a nozzle diameter of 2 mm. The surface temperature and heat flux are estimated by applying two-dimensional inverse solution to the measured temperatures in the block during the quench and then the flow configuration on the surface during the quench is synchronously observed with a high speed video. As a result, the changes in the surface temperature and in the surface heat flux are clearly shown with movement of the wetting front. The resident time at which the wetting front starts spreading after the impingement of jet can be predicted by a proposed correlation. The fundamental character of how the surface temperature and heat flux change with the wetting front, can be understood.

Keywords:. Two-dimensional transient cooling, Quenching, Wetting front, Inverse solution, Impinging Jet Heat conduction

1. INTRODUCTION

Many researches [1 – 20] have been extensively conducted about heat transfer during quenching a high temperature solid with a liquid, since the quenching phenomenon has been commonly encountered in industrial applications such as a continuous casting [1], a strip steel [2, 3] on a run-out table, forging and a rewetting process [13, 14] in an emergency cooling of fuel elements related to a safety of the reactor in a water-cooled nuclear reactor during a loss of-coolant accident (LOCA). This cooling process becomes extremely complicated due to the change of the heat transfer mode from film boiling, transition boiling, nucleate boiling and then single-phase heat transfer with time. In addition to these, these modes can coexist on the high temperature surface and have a large difference in heat transfer rate. Therefore, whether the surface is wetted or not has a large influence on the heat transfer rate during the quench. It is very important to understand the change in the surface temperature and heat flux and to predict the wetting front during the quenching. The experimental conditions related to the quench are summarized in Table 1.

As for researches on a speed of wetting front and a progress in wetting front, a study of rewetting of the core rod were made using a falling liquid film along the rod related to the safety of nuclear reactor in the emergency cooling and a correlation to predict wetting velocity was proposed [14]. However, in the rewetting of the core rod, analytical method became relatively easy, because no coupling between solid and falling liquid was taken into account due to a negligible small heat capacity of the rod. Nevertheless, a correlation to predict the wetting condition and the wetting velocity correctly seems to be not proposed, yet. A model was proposed based on the coupling problem between heat conduction in a high temperature solid and heat transfer in a cooling liquid. This model [17] needs an assumption for the cooled surface, for example, the heat transfer coefficient distribution, the heat flux distribution or a temperature at which the wetting takes place. Ohtake et al. [17] employed heat transfer characteristics in pool boiling and proposed their model to predict the wetting velocity during the quench based on two-dimensional unsteady heat conduction. No verification was provided for the boundary condition during the advancement of the wetting front.

Several experimental and analytical investigations [1, 2, 3, 14, 16, 19, 20] had been conducted to understand film boiling heat transfer of water jets impinging on high temperature flat plates in the jet stagnation zone and to control the surface temperature. Filipovic et al. [1] studied the regimes of boiling for quenching phenomena by using nickel-plate copper, which was preheated to an initial temperature exceeding 700°C and, subsequently, quenched with a water wall jet. They found that the front was at the leading edge of transition boiling zone and was approximately coincident with location of the maximum heat flux. They succeeded in showing qualitative trend in heat transfer characteristics during the quench. How the surface temperature and heat flux change with the movement of the wetting front is not clear, yet, since a procedure to estimate the surface temperature and heat flux is not established, commonly. In other words, the procedure needs an inverse solution to estimate the surface temperature and heat flux within accepted error level.

Mitsutake and Monde [18] made an experiment on a quench of a high temperature solid with an impinging jet and showed an effect of jet velocity, thermal properties of solid and subcooling of liquid on the wetting velocity and then the change in the surface temperature and heat flux with the wetting front. The estimated surface temperature and heat flux are relatively rough because their inverse solution stood on a numerical method. Therefore, more precise discussion on relationship between heat transfer characteristics and flow situation on the cooled surface seems to be still left.

Recently, the analytical method for two-dimensional inverse heat conduction problems, IHCP, which was developed by Monde et al. [21-23], makes it possible to successfully estimate surface temperature and heat flux from the measured temperatures in the solid. Monde et al. [21], for example, determined the surface temperature and heat flux analytically for a homogeneous rectangular body, and could predict them well over the whole surface with an error less than a few percent. Hammad et al. [24] applied the same analytical solution of Monde et al. [21] to determine the surface temperature and heat flux for a cylindrical body and showed good estimation can be obtained similar to the rectangular case.

Incidentally, the quench using the impinging jet is much attractive from viewpoint of engineering and fundamental aspects as: (1) this cooling system is widely used to give high heat transfer rate and high critical heat flux, (2) the flow situation on the surface becomes one dimension and (3) the experiment becomes simpler than other geometrical configurations. Therefore, we choose the jet impinging system for cooling the high temperature surface.

In the present research, we measured the temperatures in the high temperature cylindrical body during the quench of it with the impinging jet and we therefrom estimate the surface temperature and heat flux by applying the inverse solution developed by Monde et al. [21- 26]. A high speed video camera observed the propagation of the temperature wetting front and boiling region flow over the hot surface at the same time of the measurement. The estimated surface heat condition, which is based on the measured temperatures inside the heated body, in conjunction with the observation made to the movement of liquid on the surface allowed us to better understand the quenching phenomena. The main objective of the present research is to (1) predict when the wetting front starts going forward after the jet impingement, (2) determine the surface temperature and heat flux, (3) measure the boiling region and wetting front which move with time, and (4) find the positions at which the maximum heat flux and maximum heat transfer coefficient occur.

2. EXPERIMENTAL APPARATUS AND PROCEDURE

2.1 Experimental Apparatus

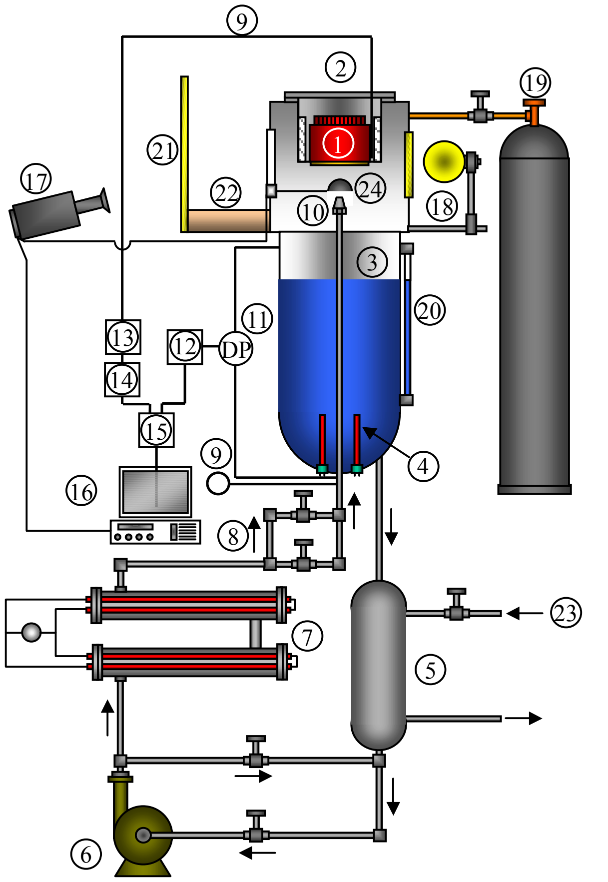

1.Tested block, 2.Block holder, 3.Liquid tank, 4.Heater, 5.Cooling jacket, 6.Pump, 7. Auxiliary heater, 8.Regulating valve, 9.Thermocouple, 10.Nozzle, 11.Differential pressure, 12.Dynamic strain meter, 13.Ice box, 14.Voltage amplifier, 15.A/D converter, 16.Computer, 17.High-speed video camera, 18.Spot light, 19.Nitrogen cylinder, 20.Level gauge, 21.Glass frame, 22.Vessel, 23.Cooling water, 24.Rotary shutter Tested block

Fig.1 Schematic of experimental apparatus

The experimental apparatus, as shown in Fig.1, consists of four major parts; a) Heated block capsule, b) Liquid circulation system c) Data acquisition system, and d) High-speed video camera.

The experimental procedure is accomplished as follows: The water container (3) is filled with distilled water up to a certain level which is observed by the level gauge (20). Water fills all the pipelines up to the pump inlet. The regenerative pump (6), then, pumps the water so that it exits out of the nozzle (10). The position of the nozzle is fixed by an adjustable device in such a way that the water jet (10) can strike exactly at the center of the block (1). A shutter (24) is mounted in front of the nozzle to prevent water from striking the block (1) prematurely and to maintain a constant water temperature by forcing it to run within a closed loop system. The desired temperature of the water is obtained by controlling the main heater (4) and auxiliary heater (7). The initial temperature of the block (1) is achieved by heating it with an electrical heater mounted around the block. The jet velocity is adjusted by a regulating valve (8). Nitrogen gas is fed around the heated surface block by opening the cylinder valve (19) to remove oxygen away from the heated surface and, consequently, prevent oxidization from taking place. When all the desired experimental conditions are fulfilled then the shutter (24) is opened for the water jet to strike the center of the heated block. The high speed video camera (17) starts to record the flow aspect over the heated block surface and then at the same time, the 16 thermocouples also start measuring the temperatures inside the heated block.

In this experimental work we will mainly discus the characteristic of heat transfer for the brass as the material for the heated block except for the time when the wetting front start going forwards after the jet impingement will be discussed. The block is initially and uniformly heated to about 300°C. The jet water is subcooled at ΔT_{sub} = 50 K with a jet velocity, u, of 5 m/s and 2 mm nozzle diameter.

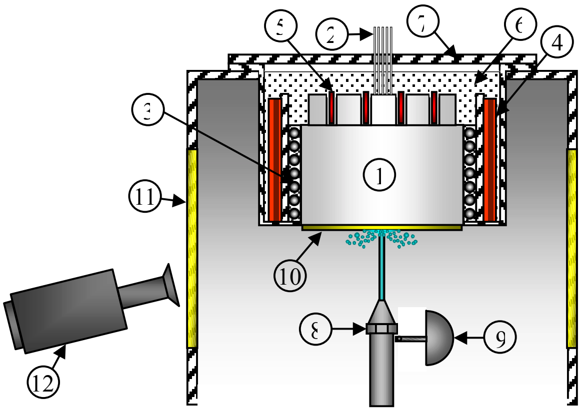

1.Tested block, 2.Thermocouples, 3.Sheath heater, 4.Band type heater, 5.Slot type heater, 6.Glass wool, 7.Block holder, 8.Nozzle, 9.Rotary shutter, 10.Hot surface, 11.Glass window, 12.High Speed video camera

Fig.2 Schematic of main part of experimental apparatus

2.2 Heated Block

The heated block is of cylindrical shape with 94 mm diameter and 59 mm height. In order to make it easy to fix the thermocouples inside the heated block, a part of it was removed along the vertical axis until 1.5 mm from the heated surface. This effect of removal appears in an area more than r = 30 mm, where it is found from a video observation that a symmetrical expanding of the wetting front collapses. Therefore, an available region in which the quench is correctly done becomes less than r = 30 mm. Sixteen thermocouples (CA-type, 1 mm sheath diameter and 0.1 mm wire diameter) are located at two different depths of 2.1 mm and 5 mm from the surface. At each depth, eight thermocouples are inserted along the r-axis. To protect the boiling surface from oxidation, the block surface was coated with a thin layer of gold, 16 μm, which has an excellent oxidation resistance characteristic and also a good thermal conductivity; $k \approx 317$ W/m/k. The surface roughness is 0.2~ 0.4 μm. Figure 2 shows the assembly of the block, where it is mounted in a block holder and is heated by an electrical sheath heater with 0.94 kW capacity, that is coiled around the block circumference. To thermally insulate the block and to keep a uniform heat flux at the surfaces, two auxiliary heaters are used; one of them is of band type, 0.65 kW, and is placed around the block circumference, while the second is of slot type, 0.5 kW, and is placed in the four groves in the upper part of the block as illustrated in Fig. 2.

2.3 Data Acquisition System

The thermocouples are scanned sequentially at 0.05 second intervals, with 8.0 ms needed to read all of the thermocouples using 16-bit resolution with an analog-digital converter. The duration of the total data acquisition period depends on parameters such as the impingement velocity, u, subcooled temperature, ΔT_{sub}, block initial temperature, T_{block}, and type of block material. The uncertainty in the temperature measurements is ±0.1°C, while the uncertainty in the placement of the thermocouples is estimated to be ±0.1 mm. The time lag for the response of the thermocouples is estimated to be less than 0.1 sec.

2.4 Visual Observation

Flow aspect during the quenching of the heated surface was recorded using a high-speed video camera. This camera is capable of recording pictures with a resolution of 572×434 pixels and has a maximum frame rate of 12400 frames/second. The video images were divided into pictures for short interval of time to allow us to measure the observed wetting front and transition boiling positions. The error in this measurement is ±0.18 mm.

3. ESTIMATION OF SURFACE TEMPERATURE AND HEAT FLUX

3.1 Procedure for Calculating Surface Temperature and Heat Flux

The every eight temperatures are measured along r-direction at the depths of 2.1 and 5 mm in the heated block. A procedure based the inverse solution proposed by Monde et al. [21] and Hammad et al. [24] makes the calculation of the surface temperature and heat flux from measured temperatures possible. Equations (1) and (2) are the inverse solutions to calculate them.

For the surface temperature,

$$\theta_w(\xi,\tau) = \sum_{j=0}^{N_j}\sum_{k=-1}^{N} \frac{G_{j,k}^{(1,2)} J_0(m_j\xi)}{\Gamma(k/2+1)}(\tau-\tau_1^*)^{k/2}$$
$$+ \sum_{j=0}^{N_j}\sum_{k=-1}^{N} \frac{G_{j,k}^{(2,1)} J_0(m_j\xi)}{\Gamma(k/2+1)}(\tau-\tau_2^*)^{k/2} \qquad (1)$$

and for the surface heat flux,

$$\Phi_w(\xi,\tau)=\sum_{j=0}^{N_j}\sum_{k=-1}^{N}\frac{H_{j,k}^{(1,2)}J_0(m_j\xi)}{\Gamma(k/2+1)}(\tau-\tau_1^*)^{k/2}$$
$$-\sum_{j=0}^{N_j}\sum_{k=-1}^{N}\frac{H_{j,k}^{(2,1)}J_0(m_j\xi)}{\Gamma(k/2+1)}(\tau-\tau_2^*)^{k/2} \quad (2)$$

All calculations were first performed by converting the measured temperatures into non-dimensional ones.

According to Monde et al. [21], the numbers of terms, N = 5 and N_j = 28 in Eqs. (1) and (2) are enough to estimate them. The coefficients in Eqs. (1) and (2) are related to the measured temperatures. The details of the process to derive the coefficients are given in the work of Hammad et al. [24].

3.2 Approximate Equation for Measured Temperatures

The number of N_j = 28 in Eqs. (1) and (2), which is related to the number of eigenvalues needs more than 29 measuring points for the each depth in the solid. It is actually difficult to settle these number of the measuring points in the solid. Recently, Monde et al. [22] showed based on a numerical discussion that the number of the measuring points is eight enough in case that the third order Spline interpolation is applied. The temperatures are measured at the eight points for the each depth and the temperatures at other needed points are estimated using the Spline interpolation. A trial function to approximate the temperatures at these points can be given as follows:

$$f(\xi,\eta_n,\tau)=\sum_{j=0}^{N_j}J_0(m_j\xi)\sum_{k=1}^{N}\frac{D_{j,k}^{(n)}}{\Gamma(k/2+1)}(\tau-\tau_n^*)^{k/2}$$
$$n = 1, 2 \qquad (3)$$

The reason why this trial function is selected is that the eigen function, Jo($m_j\xi$), always satisfies the given boundary conditions at ξ = 0 and 1 and the half polynomial function for the time constitutes one of a general solution for heat conduction equation and then Monde [26] showed that the half polynomial function is suitable for one-dimensional case.

The coefficients, $D_{j,k}^{(n)}$ in Eq.(3) are determined from the measured temperatures using the least mean square method.

3.3 Measured Temperature

Figure 3 shows, for example, the measured temperatures at four different locations on the depth of z_1 = 2.1 mm for brass and copper. How to calculate the the coefficients, $D_{j,k}^{(1)}$ in Eq. (3) is explained here, and the details concerned with heat transfer will be discussed later.

We first calculate the needed temperatures at several different positions from the eight actual measured temperatures at the eight measured points on the depth of z_1 = 2.1 mm for example, for a jet velocity of u = 5 m/s, a subcooling of ΔT_{sub} = 50 K using the third order Spline interpolation. We can determine the coefficients, $D_{j,k}^{(1)}$ in Eq. (3) from the measured and calculated temperatures using least mean square method. Figure 4 shows the surface temperature variation reproduced by Eq. (3) with the determined coefficients, $D_{j,k}^{(1)}$.

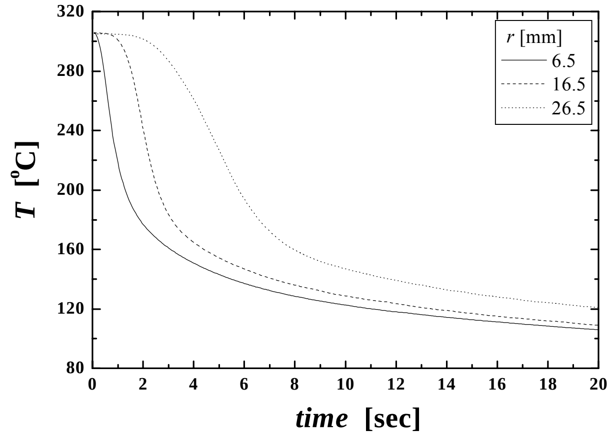

(a) Brass, T_b = 300°C, T_{liq} = 50 °C, u = 5m/s

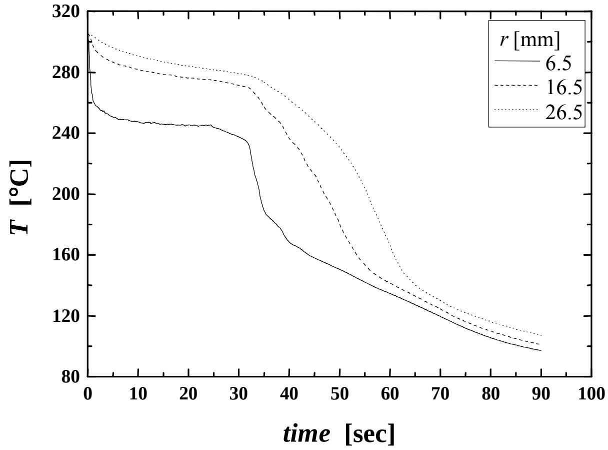

(b) Copper, T_b = 300°C, T_{liq} = 50 °C, u = 5m/s

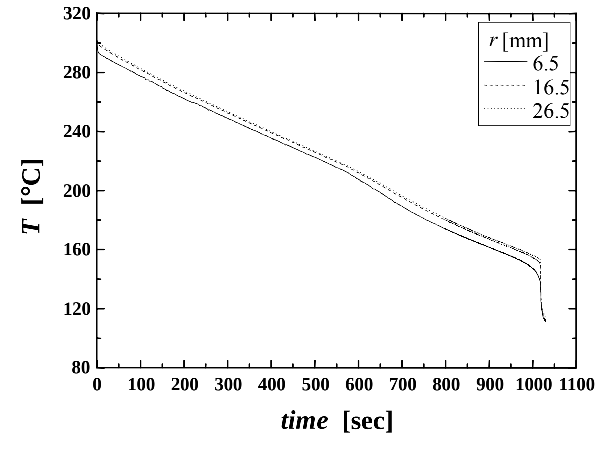

(c) Copper, T_b = 300°C, T_{liq} = 95 °C, u = 5m/s

Fig.4 Cooling curves for brass and copper

It should be mention to obtain Eq. (3) that in the case that the temperatures along the r-direction sharply drop and the point of the temperature drop moves toward outside with time, Eq. (3) usually fails to approximate the temperature change over the whole time and the domain with high accuracy. For this case, one first divides the whole time into several subdivisions of time and then determines Eq.(3) for each subdivision. As the result, Eq. (3) can approximate the temperature change within an error of 1 % compared with the measured temperature, although a comparison between them is omitted here. Monde et al. [23] numerically verified that this method is effective not only for Eq. (3) approximating the sharp temperature change well but also for improvement of the inverse solution.

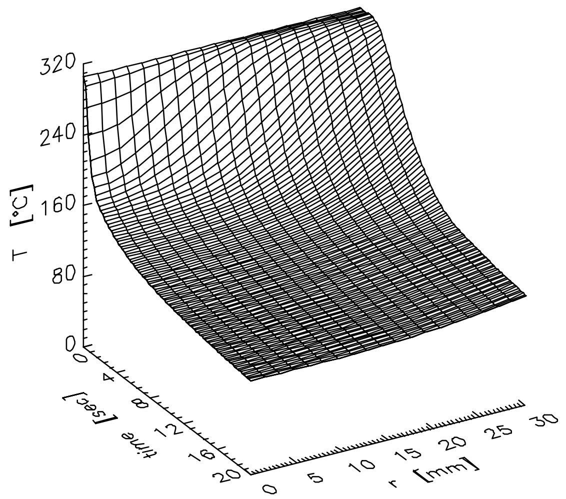

Fig. 4 Temperature change reproduced from the measured temperatures at z = 2.1 mm by Eq. (3) (Brass, T_b = 300°C, T_{liq} = 50 °C, u = 5m/s)

4. EXPERIMENTAL RESULT AND DISCUSSION

4.1 Cooling Curves during Quench

Figure 3 shows the change in the measured temperatures at four different position on the depth of z_1 = 2.1 mm during the quench of brass and copper at the same initial temperature of T_b = 300 ℃ at the same velocity of 5 m/s and at different subcoolings.

It is found from Figs. 3(a) and (b) that the measured temperatures behaves at different way depending between copper and brass nevertheless the other experimental parameters are the same. In addition, a comparison of Figs. 3(b) and (c) shows the different trend in the measured temperatures for the different subcooling. For the case of brass, for example, the measured temperature at the position nearest to the jet impingement, r = 6.5 mm, quickly drops immediately after the jet impingement and then the other measured temperatures start dropping following a drop in the measured temperature at the nearer position after a few second is delayed. The slope of the temperature drop is also the steepest at the measured point nearest to the center. On the other hand, for the copper, the measured temperature at r = 6.5 mm quickly drops after the jet impingement. However, the steep drop of the measured temperature changes into a gradual one at a time. The temperature suddenly drops, again. The first temperature drop is caused by direct contact with liquid by the jet impingement. During the time in which the measured temperature gradually decreases, the surface is covered with vapor blanket generated by the first impingement. The second one is caused by the establishment of wetting. After this time, the wetting front goes forwards and the temperatures at the other positions starts decreasing sharply in order of the measured location. On comparison of Fig. 3(b) and (c), the time duration when the film boiling is lasting near the impinging zone and the wetting front does not go forwards become much longer for a low subcooling of ΔT_{sub} = 5 K than that for a high subcooling of ΔT_{sub} = 50 K. However, the slops of the temperature decrease, dT/dt, at the measured positions for ΔT_{sub} = 5 K becomes slightly different from those for ΔT_{sub} = 50 K, although the levels of the temperature drop are largely different. The temperature drops are nearly 140 K and 160 K for the case of ΔT_{sub} = 5 K.

The time when the wetting front goes forwards is very important to evaluate the heat transfer rate from the high temperature surface into liquid, since it is much different depending on whether the surface is wetted or not. This time may be called the resident time, t*.

The time is automatically counted when the shutter is rotated and the jet starts impinging on the surface in the experiment. The characteristics of heat transfer are largely different between before and after the resident time. Before the resident time, an effect of jet impingement on the heat transfer is limited near the impinging zone. After the resident time, the jet influences the heat transfer over the surface. The heat transfer after the resident time will be discussed and the time will be reset zero at the time resident time at which the wetting front goes forwards.

4.2 Resident Time

Figure 5 shows the resident time occurring for the various experimental conditions. The result for the resident times more than 4 second are given in Fig. 6, since the cases for t* < 4 sec can be judged as the instant movement of the wetting front.

Figure 5 shows that for the case of the subcooling, ΔT_{sub} = 80 K, the wetting front instantly goes forward as shown in Fig. 3(a) after the jet impingement for any condition of jet velocity, u, and the initial temperature, T_b, namely t* = 0. For the case of steel, the resident time appears only for the condition of u = 3 m/s and ΔT_{sub} = 5 K. For the case of copper, the wetting front hardly goes forward after the jet impingement among three materials.

Figure 6 shows the measured resident time plotted against the jet velocity. It is found from Fig. 6 that for the extreme case of T_b = 300 °C, ΔT_{sub} = 5 K, u = 3 m/s and copper, the resident time reaches about half hour. During the resident time, the surface is covered with the vapor under the impinging zone, in which the wetting point is observed to be fluctuating violently around influential area of jet and then the surface temperature gradually drops over the cooled surface by film boiling and heat conduction. Figure 7 shows that the resident time increases with a decrease in the jet velocity and also increases in order of steel, brass and copper for the same condition.

In order to discuss an effect of the subcooling, jet velocity and initial temperature on the resident time, we tentatively assume that the wetting front does not go forward during a balance of heat transfer from solid to liquid, that is q_l is equal to q_s. The heat flux transferred from the solid through heat conduction can be approximated as:

$$q = -\lambda_s \frac{\partial T}{\partial x} \approx \lambda_s \frac{\Delta T}{\Delta x} = \lambda_s \frac{\Delta T}{\delta_t} = \frac{(T_b - T_w(t))}{\alpha\sqrt{t/(\rho c \lambda)_s}} \tag{4}$$

On the other hand, the heat transfer for the liquid can be given as $q_l = h(T_w(t) - T_{liq})$, where h is a heat transfer coefficient and may be a function of liquid velocity and superheat of heated surface. From $q_l = q_s$, one may obtained the following equation,

$$\sqrt{(\rho c \lambda)_s / t^*} = \alpha \frac{q_s}{(T_b - T_w)} = f(u, (T_b - T_l), (T_{sat} - T_l)) \tag{5}$$

where $\beta = \sqrt{(\rho c \lambda)_s/(\rho c \lambda)_l}$ and a is a constant depending on the level of temperature penetration into the solid. The heat transfer coefficient is generally a function of the jet velocity and the temperature differences of $(T_w(t) - T_{liq})$, which may be related to $(T_b - T_{liq})$ and $(T_{sat} - T_{liq})$.

Figure 7 shows the resident time plotted against a combination of u, $(T_b - T_{liq})$ and $(T_{sat} - T_{liq})$ and expresses the following equation, which can be determined by the least mean square method.

$$\sqrt{(\rho c \lambda)_s / t^*} = 1.1x10^5 \{u^{0.5}(T_{sat} - T_{liq})^{0.5} / (T_b - T_{liq})^2\}^{1.27} \tag{6}$$

It is found from Fig. 7 that the resident time for any material of carbon steel, brass and copper can be predicted except for a couple of data in a range of $t^* < 100$ sec by Eq. (6). In addition, the left hand side in Eq. (5) can be considered to forecast the heat conduction in the solid correctly during the quench.

4.3 Surface Temperature and Heat Flux

Figures 8 and 9 show the surface temperature and the surface heat flux estimated by Eqs. (1) and (2), where the coefficients in Eq. (3) are previously determined from the measured temperatures at the depths of 2.1 and 5 mm (for example, see Fig.3). In Figs. 8 and 9, the surface temperature at q_{max} and the track of the maximum surface heat flux, q_{max}, are shown by a solid line on the surface temperature and heat flux planes. In addition, the tracks of the maximum heat flux, r_q, and the observed wetting front, r_w, are plotted against time on the *r-t* plane by a solid line and dashed line, respectively. Figure 8 shows that the surface temperature sharply drops near the wetting front and then the position of the sharp temperature drop moves with the wetting front. The surface temperature at the maximum heat flux appears near the point turning from the sharp drop into a gradual decrease and almost falls in the range of 140 ~168°C. This trend was already pointed out in previous studies [2] of quenching the hot surface, although the detail relation ship between the surface temperature and heat flux was not discussed, for example the surface temperature at

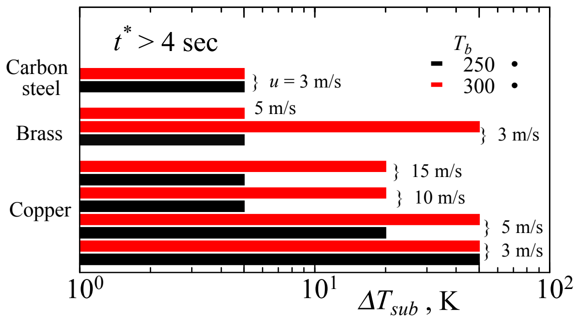

Fig. 5 Resident time, t* at which wetting location goes forwards

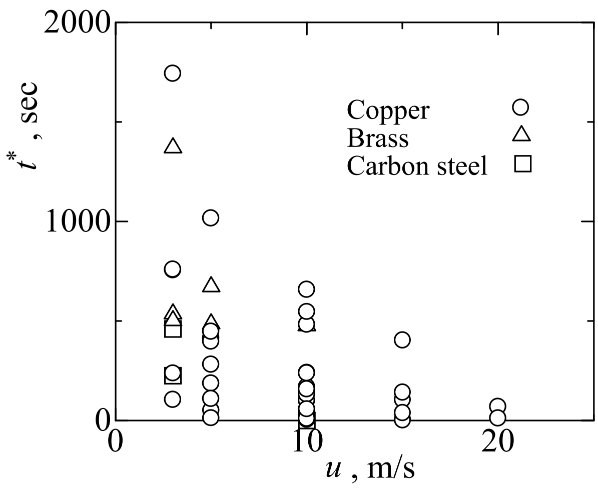

Fig. 6 Relationship between resident time and jet velocity

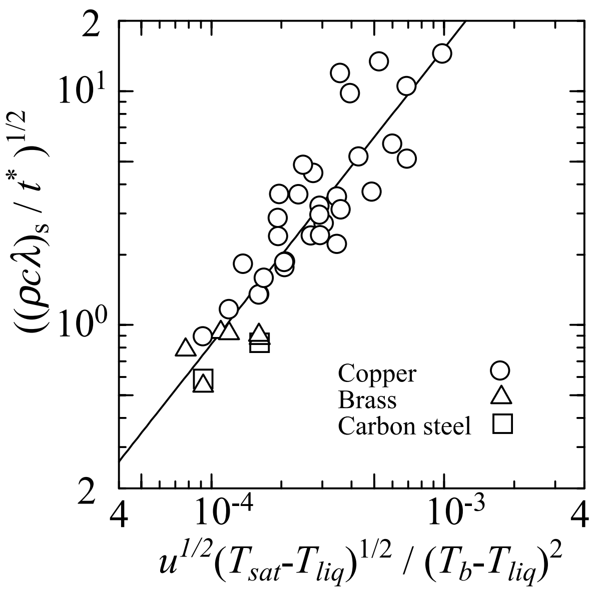

Fig. 7 Correlation of resident time

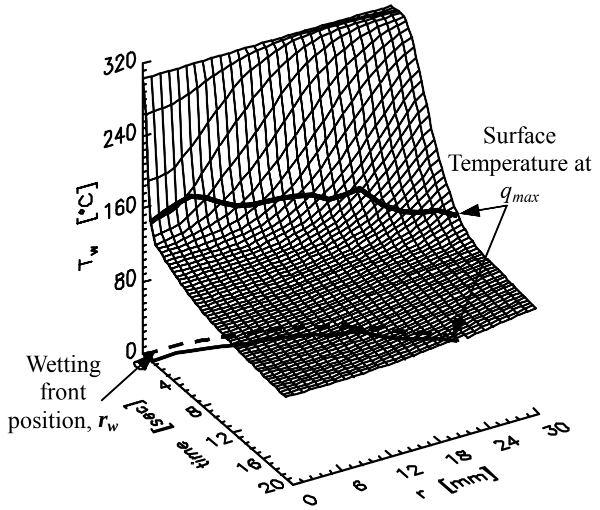

Fig. 8 Estimated surface temperature from Eq. (1)

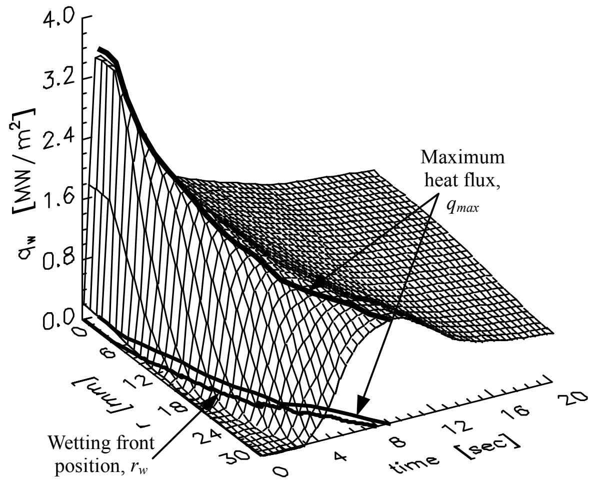

Fig. 9 Estimated surface heat flux from Eq. (2)

q_{max} becomes in the range of 140 ~168°C. Figure 9 shows that the maximum heat flux gradually decreases along the r-direction and the position of q_{max} appears behind the wetting front.

4.4 Flow Situation and Characteristics of Cooling

Figure 10 shows an observed flow situation on the cooled surface, for example, at the time of t = 2.7 sec and the distributions of the surface temperature and heat flux and heat transfer coefficient ($h_s = q_w(t)/(T_w(t) - T_{liq})$ at the same time along the r-direction. In addition, for a comparison of transient heat transfer coefficient, the steady state heat transfer coefficient ($h_s = q/(T_w - T_{liq})$) for single-phase flow is calculated from the correlation proposed by Liu et al. [27], which was derived for the constant heat flux and the temperature of jet liquid as reference.

In Fig. 10, some specific points are pointed out, for example, the point, r_w, at which the hot surface is observed to be wetted by the liquid, and the point, r_s, at which the generated vapor and splashed droplets can not be observed, and the point, r_q, at which the estimated heat flux becomes maximum.

We can recognize three regimes in the flow situation apparently from the image in Fig. 10: the first is no splashed droplets, the second is splashed droplets generated by strong vapor ejection, and the third is disappearance of the droplets, that is the dry area. The boundaries of the three regimes can be identified at the locations of r_s and r_w. The position of r_w can be called the wetting front.

Figure 10 shows that the surface temperature drops linearly and largely just before the wetting front, while the position of the maximum heat flux appears in the region where no splashed droplets is observed, that is behind the position of r_s. The heat flow occurs along r-direction in the region where the wetting front does not reach due to the linear decrease in the surface temperature along r-direction. In the region between the locations of r_s and r_w, the heat flux sharply decreases, and the surface temperature inversely increases. Therefore, the heat transfer mode in this region may shift from nucleate boiling to film boiling along r-direction. On the observation of Fig. 10, the nucleate boiling disappears at the position of r_w and the dry area continues beyond the position of r_w. The heat transfer rate in the region of $r_s < r < r_w$ changes depending on the ratio of nucleate boiling and film boiling. The heat transfer coefficient starts decreasing slightly before the position of r_q. This is due to the fact that the heat flux changes mild around the position of r_q, while the surface temperature starts increasing there.

Figure 10 shows the position of r_q appears in the region of $r < r_s$. As the result, it is natural to consider that nucleate boiling surely takes place in the region of $r < r_s$ and the generated vapor there is sudden condensed by the subcooled liquid and no net generated vapor is apparently observed. The net generated vapor can be first observed at the position, r_s. The position at which nucleate boiling starts occurring might be near the position at which the value of h becomes larger than the value of h_s. In the region of $r_q < r < r_s$, the subcooled liquid receives a large amount of heat from the surface and its temperature is raised, and also the surface temperature starts increasing.

In the region of $r_s < r < r_w$, the liquid on the surface may almost reach the saturation temperature and the evaporation there becomes violently due to the evaporation on triple phase lines [28], by which most of liquid is splashed away. In this region, the dry area appears on the surface and a fraction of this dry area would be enlarged with an advance in the transition from nucleate boiling to film. Most of liquid is finally splashed away. However, the heat flux of q_w = 1.5 MW/m^2 at $r = r_w$ is still high enough and then the surface temperature of about T_w = 190 ℃ is kept. Therefore, a few liquid is considered to still remains on the surface. In the region of $r > r_w$, non-wetted area appears and its temperature is also increased enough.

Recalling the flow situation in the region of $r < r_s$, that no splashed net droplets is observed and the heat transfer coefficient is larger than the steady state heat transfer coefficient predicted by Liu et al. [27] except for the impinging zone, vapor is surely generated, but these vapor is suddenly condensed by the subcooled liquid resulting into no net vapor generation. Incidentally, Kandlikar [29] pointed out that in the case of subcooled flow boiling in tube, the position of net vapor generation is behind the position at which the actual boiling is initiated. Finally, the heat transfer coefficients in r_s < r < r_w, becomes smaller than that for single phase heat transfer.

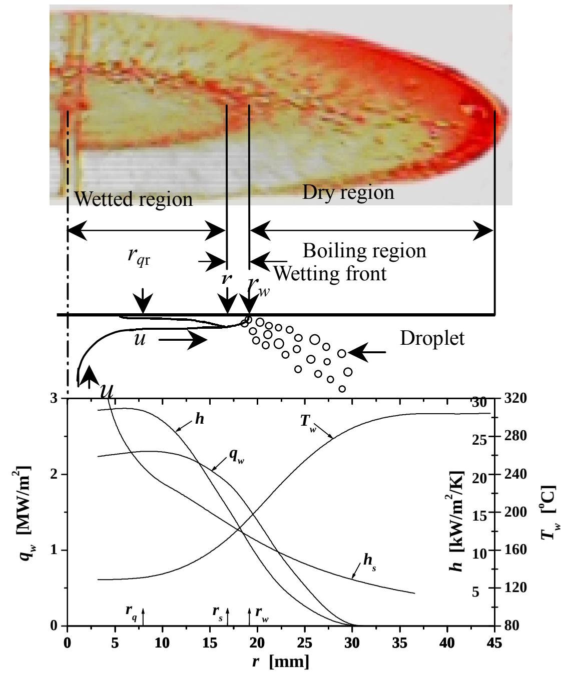

Fig. 10 Relationship between flow configuration and surface temperature and heat flux distributions at t = 2.7 sec (Brass, T_b = 300 °C, T_{liq} = 50 °C, u = 5m/s)

4.5 Change in Cooling Characteristics along r-direction

Figure 11 shows the positions of r_w, r_s, r_q and the position r_h at which the maximum heat transfer coefficient h_{max} takes place move on the surface along the r-direction with time.

Figure 11 reveals that the region of r_s < r < r_w becomes very narrow in the range of r < 15 mm and most of liquid is splashed out near the location at which the net vapor generation emerges. Beyond the location of r =15 mm, the region of r_s < r < r_w gradually becomes wide. The region of r > 20 mm, the position of r_q almost overlaps on the position of r_s. Therefore, the nucleate boiling takes place near the position of r_s even in the region of r_s < r < r_w. This is attributed to the fact that the surface is cooled down by the transition boiling and its temperature itself is below enough for the nucleate boiling to occur. In addition, another reason of occurrence of the nucleate boiling is that the effect of forced convection is weakened due to the decrease in liquid velocity and the rise in the liquid temperature.

It is found from Fig. 11 that the position, r_h, at which the maximum heat transfer coefficient appears emerges out relative large behind the position of r_q.

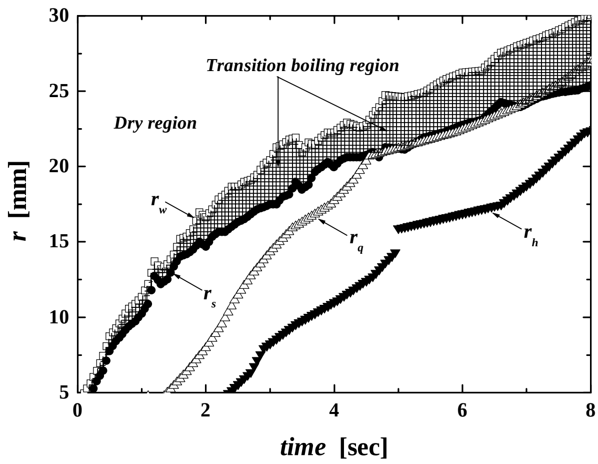

Fig. 11 Movement of positions of of r_q, r_s, r_{wet} and r_h with time (Brass, T_b = 300 °C, T_{liq} = 50 °C, u = 5m/s)

4.6 Relationship between Cooling Characteristic and Flow Situation

Figures 12, 13 and 14 shows how the surface temperatures, heat fluxes and heat transfer coefficients at a point on the cooled surface change with time, respectively. The times when the specific points of r_q, r_s, r_w, and r_h coincides at the point are marked.

Figure 12 shows the surface temperature sharply drops in the region of r ≤ 11.1 mm, and gradually decreases for r ≥ 20.6 mm. This difference between the regions of r ≤ 11.1 mm and r ≥ 20.6 mm comes from the effect of heat conduction in r-direction, that is in progress of wetting front, a heat flow in r-direction is increased. Figure 12 reveals that the maximum heat flux takes place when the surface temperature reaches below about 160 ℃ and then the maximum heat transfer coefficient appears. At the point of r = 20.6 mm, the temperature at the wetting point becomes rather low and the position of r_q appears earlier than the position of r_s. Therefore, the nucleate boiling already occurs at the position of r_s at r = 20.6 mm.

Figure 13 shows the maximum heat flux gradually decreases along the r-direction and in the region of r ≤ 8.0 mm the heat flux at r_w reaches about 1 MW/m^2 allowing us for the dry area to occupy some part on the surface. On the other hand, at the point of r = 23.8 mm the dry area instantaneously disappears immediately after the wetting front reaches there. As the result, the wetting conditions between the points of r ≤ 8.0 mm and r = 23.8 mm are quite different.

Figure 14 shows the change of the heat transfer coefficients calculated from the values of T_w and q_w shown in Figs. 12 and 13 with time. Figure 14 shows that the heat transfer coefficients approaches a certain value after passing the time at which the maximum heat transfer coefficient takes place. This fact would be attributed to the change of the heat transfer mode from boiling heat transfer to single-phase heat transfer, that is forced convection, where heat transfer coefficient is generally a function of the Reynolds number. Each value of local heat transfer coefficient after reaching the constant value decreases along r-direction. This trend comes from the fact that the heat transfer is under the forced convection heat transfer.

Figure 13 shows the distributions of heat flux and temperature along r-direction. It is seen from Fig.14 that during the time from 4 to 8 sec, the surface temperatures over the heated surface reach a temperature range, which is an appropriate temperature to generate boiling and is too low to hold a stable film boiling. On the other hand, the heat fluxes in the same time of 4 to 8 sec are almost constant in the region of $r < r_s$. Therefore, nucleate boiling heat transfer is dominant in this region. It should be note that the nucleate boiling pauses on a part of the surface where the forced heat transfer coefficient becomes larger than the boiling one, since Monde and

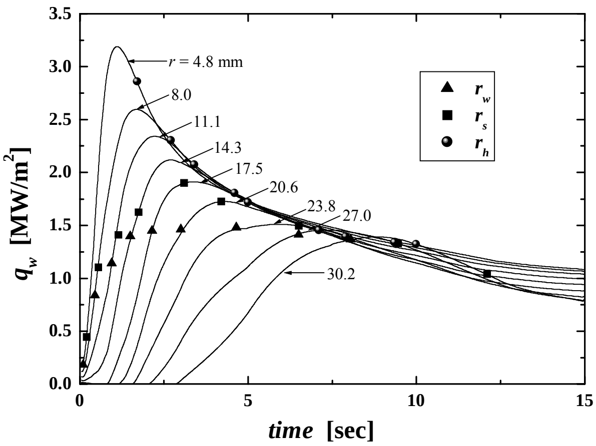

Fig. 12 Surface temperature at a location with time (Brass, T_b = 300 °C, T_{liq} = 50 °C, u = 5m/s)

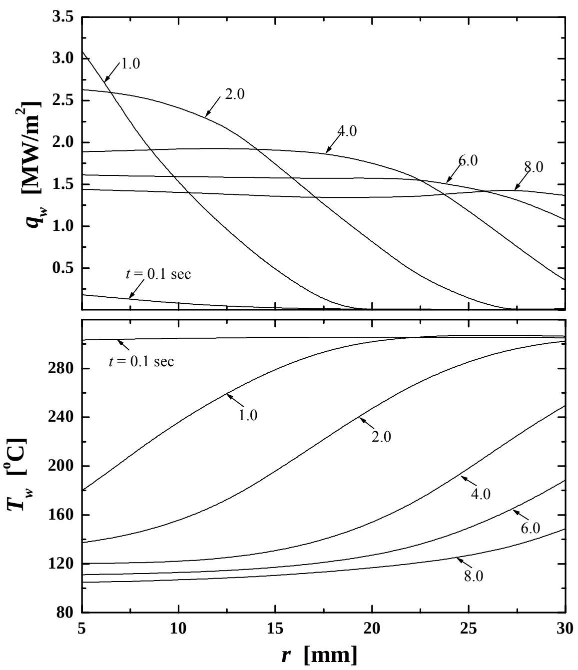

Fig. 13 Surface heat flux change at a location with time (Brass, T_b = 300 °C, T_{liq} = 50 °C, u = 5m/s)

Katto [30] reported that under the steady state condition the boiling starts taking place in the area far from the jet impingement and then the boiling area propagates inward with an increase in heat flux.

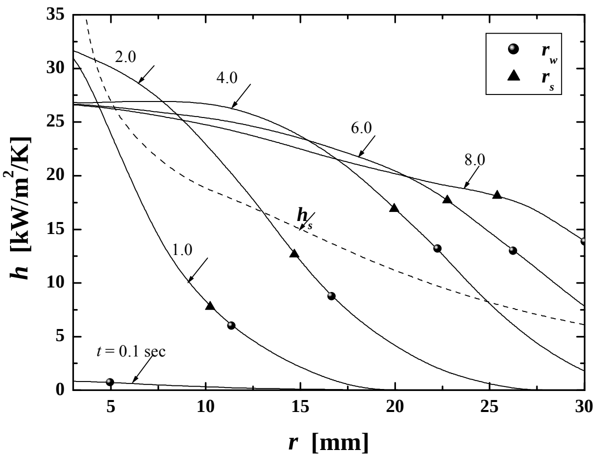

Fig. 14 Heat transfer coefficient along r-direction for a different time

(Brass, T_b = 300 °C, T_{liq} = 50 °C, u = 5m/s)

5. CONCLUSION

1. A qualitative understanding of transient heat transfer characteristic is obtained during quenching the high temperature surface with a subcooled impinging jet.
2. The wetting front does not expand for some experimental condition immediately after the jet impinges on the hot surface. There is a resident time for the wetting front to start expanding. Equation (6) to predict the resident time is proposed.
3. The positions where the maximum heat flux and maximum heat transfer coefficient take place during the quenching are qualitatively made clear.
4. The maximum heat flux appears when the surface temperature reaches below about 160 ℃

Acknowledgement

Author would like to appreciate Mr J. Hammad who has conducted this experimental study and Dr. Y. Mitsutake, supporting this study.

. REFERENCES

1. J. Filipovic, F.P. Incropera, and R. Viskanta, "Quenching phenomena associated with a water wall jet: I. Transient hydrodynamic and thermal conditions", *Experimental Heat Transfer*, 8, (1995), 97-117
2. Hatta, N., Fujimoto,H. , Takuda, H., Kinoshita, K., Collision dynamics of a water droplet impinging on a rigid surface above the Leidenfrost temperature, *International Journal of Iron and Steel Institute of Japan*, **35**, 1995, pp.50-55
3. Kokado, J., Hatta, N., Takuda, H., Harada, J., Yasuhira, N., An analysis of film boiling phenomena of subcooled water spreading radially on a hot steel

plate, *Archiv für das Eosemhüttenwessen*, **55**, 1984, pp.113-118.

4. Kumagai, S., Sano, Y., Kamata, T., Suzuki, S. and Kubo, R., Boiling Heat Transfer to an Impinging Jet in Cooling a Hot Metal Slab, *Trans. of JSME* (in Japanese), **60**-570B, (1994), 609 – 613.
5. Kumagai, S., Kawazoe, M., Suzuki, S. and Kubo, R., Transient Cooling of Hot MetalPlate with Impinging Water Jet, *Trans. of JSME* (in Japanese), **61**-590B, (1995), 3749 – 3754.
6. Hall, D.E., Incropera, F.P., Viskanta, R., Jet impingement boiling from circular free-surface jets during quenching experiments, *Proc. of the ASME Heat Transfer Division, ASME Heat Transfer Division,* (Publication) HTD, **333**-2, 1996, pp. 131-141.
7. Ueda, T., Tsunenari, S., and Koyanagi, M. , An investigation of critical heat flux and surface rewet in flow boiling system, *Int. J. Heat Mass Transfer*, 26, 8, (1983), 189-1198.
8. Ueda, T., Inoue, M., Rewetting of a hot surface by a falling liquid film - effects of liquid subcooling, *Int. J. of Heat and Mass Transfer*, **27**-7, 1984, pp.999-1005.
9. Dhir, V.K., Duffey, R.B., Catton, I., Quenching studies on a Zircaloy rod bundle, *J. of Heat Transfer*, **103**, 1981, pp.293-299.
10. Iloeje, O.C., Plummer, D.N., Rohsenow, W.M., Griffith, P., An investigation of the collapse and surface rewet in film boiling in forced vertical flow, *J. of Heat Transfer*, **97**, 1975, pp.166-172.
11. Chan, A.M.C., Banerjee, S., Refilling and rewetting of a hot horizontal tube Part I: Experiments, *J. of Heat Transfer*, **103**, 1981, pp.281-286.
12. Ohkubo, H. and Nishio, S., Transient Heat Transfer Characteristics of Mist Cooling from Horizontal Upward-Facing Surface, *Trans. of JSME* (in Japanese), **57**-539B, (1991), 2349-2354.
13. Yamanouchi, A., Effect of core spray cooling in transient state after loss-of-coolant accident, *Nuclear Science and Technology*, 5, (1968), 547-558.
14. Yoshioka, K. and Hasegawa, S., A correlation in displacement velocity of liquid film boundary formed on a heated vertical surface in emergency cooling, *J. of Nuclear Science and Technology*, 7, (1970), 418-425.
15. Dua, S. S. and Tien, C. L., Two-dimensional analysis of conduction – controlled rewetting with precursory cooling, *J. of Heat Transfer*, 98, (1976), 407-413.
16. Sun, K. H., Dix, G. E. and Tien, C.,L., Effect of precursory cooling on falling – film rewetting, *J. of Heat Transf.*, **97**-3(1975), 360-365.
17. Ohtake, H., Koizumi, Y. and Takahasih, A., Study of rewetting of vertical-hot thick surface by a falling film, *Trans. of JAME* (in Japanese), 64, 624B, (1998), 2547-2555.
18. Mitsutake, Y. and Monde, M., Heat transfer during transient cooling of high temerature surface with an impinging jet, *Heat and Mass Transfer*, 37, (2001), 321-328.
19. Liu, Z., H. and Wang, J., "Study on the film boiling heat transfer of water jet impinging on high temperature flat plate", *Int. J. Heat Mass Transfer*, 44 (2001), 2475-2481.
20. Timm, W., Weinzierl, K. and Leipertz, A., "Heat transfer in subcooled jet impingement boiling at high wall temperature", *Int. J. Heat Mass Transfer*, 46 (2003), 1385-1393.
21. M. Monde, H. Arima, W. Liu, Y. Mitsutake, and J. Hammad, "An analytical solution for two-dimensional inverse heat conduction problems using Laplace transform", *Int. J. Heat Mass Transfer*, 46 (2003), 2135-2148.
22. M. Monde, H. Arima, W. Liu, Y. Mitsutake, and J. Hammad, "An analytical solution for two-dimensional inverse heat conduction problems using Laplace transform (Effect of Measuring Point number)", *Heat transfer-Japanese Research*, (in press).
23. M. Monde, W. Liu, H. Arima, Y. Mitsutake, and J. Hammad, Improvement of Inverse Heat Conduction using Laplace transformation (Method of Partial Divition of time) *Heat transfer-Japanese Research*, (in press).
24. J. Hammad, M. Monde, H. Arima, and Y. Mitsutake, "Determination of Surface Temperature and Heat Flux Using Inverse Solution for Two Dimensional Heat Conduction", *Thermal Science & Engineering*, Vol.10 No.2, (2002), 17-26.
25. Monde, M. and Katto, Y., Bournout in a high heat-flux boiling system with an impinging jet, *Int. J., Heat Mass Transfer*, 21, 3. (1978), 295-305.
26. Monde M., Analytical Method in Inverse Heat Transfer Problem Using Laplace Transform Technique, *Int. J. Heat Mass Transfer*, Vol. 43, No. 21, (2000) pp.3965-3975.
27. Liu., X, Lienhard, J. H. and Lombara, J. S., "Convective Heat Transfer by Impingement of Circular Liquid Jets", *J. of Heat Transfer*, 113, (1991), 571-582
28. Nishio, S. and Tanaka, H., Visualization of Boiling Structures in High Heat-Flux Pool Boiling, *Trans. of JSME* (in Japanese), 69 - 682B, (2003), 1425-1432.
29. Kandlikar, S. G., Heat transfer characteristics in partial boiling, fully developed boiling and significant void flow regions of subcooled flow boiling, *J. of Heat Transfer*, 120, 2, (1998), 395-401.
30. Monde, M. and Katto, Y., Bournout in a high heat-flux boiling system with an impinging jet, *Int. J., Heat Mass Transfer*, 21, 3. (1978), 295-305.

NOMENCLATURE

Symbol	Meaning	Unit
	thermal diffusivity	m^2/s
$f(\xi, \eta_n, \tau)$	function for approximating temperature on plane $\xi = \xi_{,n}$ inside solid	
$G_{j,k}^{(m,n)}$	coefficients in Eq.(1)	
$H_{j,k}^{(m,n)}$	coefficients in Eq.(2)	

h	heat transfer coefficient, ($h = q_w / (T_w - T_{liq})$)	kW/ m^2/K
h_{max}	maximum heat transfer coefficient	kW/ m^2/K
h_s	heat transfer coefficient in steady state condition predicted by Liu	kW/ m^2/K
$J_0(r)$, $J_1(r)$	Bessel function	
Lz	Cylinder height	mm
m_j	eigenvalue (root of $J_1(m_j) = 0$)	
N	degree of approximate polynomial	
N_j	degree of eigenvalue	
$D_{j,k}^{(n)}$	coefficients derived from measured temperature	
q_{max}	maximum heat flux	MW/ m^2
q_w	surface heat flux	MW/ m^2
R_o	radius of heated block cylinder	mm
r	radial coordinate	
r_h	position for maximum heat transfer coefficient	mm
r_w	position for wetting front	mm
r_q	location at maximum heat flux	mm
r_s	location at occurrence of splashed droplets	mm
t	Time	sec
T_b	initial temperature of block	°C
T_{liq}	liquid temperature	°C
ΔT_{sub}	subcooled temperature	K
T_w	surface temperature	°C
u	jet velocity	m/s
Z_1, z_2	the distance of thermocouples location from the hot surface	mm
Φ_w	non-dimensional surface heat flux ($= qR_o/(\lambda(T_b - T_{liq})$)	
θ_w	non-dimensional surface temperature ($= (T - T_b)/T_b$)	
τ	non-dimensional time ($= at/R_o^2$)	
τ_n^*	non-dimensional time lag	
ξ	non-dimensional distance in r direction	
η	non-dimensional distance in z direction	

Table 1 Experimental conditions and geometrical configurations

Researcher	Pressure and coolant	Configuration	Liquid velocity	Jet diameter	Jet temp.	Initial temp.	Material	Configuration and dimensions
Filipovic et al.[1]	0.1 MPa Water	Laminar cooling	2 4 m/s	-	25 55 •	850 •	Oxygen free copper	Block width 38.1mm,length 508mm,height 25.2mm
Hatta et al.[2]	0.1 MPa Water	Circular impinging jet	0.1 7 L/min	10mm	20 •	900 •	18-8stainless steel	Horizontal square plate 200*200mm,t 10mm
Kokado et al.[3]	0.1 MPa Water	Circular impinging jet	0.1 7 L/min	10mm	20 90 •	900 •	18-8stainless steel	Horizontal square plate 200*200mm,t 10mm
Kumatani et al.[4, 5]	0.1MPa Water	Two dimensional flat impinging jet	1.5 3.5 m/s	2*28mm	50 100 •	390 •	Copper	Horizontal rectangle plate width 20mm,length 150mm height 120mm
Hall et al.[6]	0.1MPa Water	Circular impinging jet	2 4 m/s	5.1mm	25 •	500 800 •	Copper	Horizontal circular plate Φ112mm*t 25.4mm
Ueta et al.[7, 8]	0.1MPa R113	Falling liquid film out of tube		-	7.6 42.6 •	140 220 •	SUS304	Vertical tube O.D.Φ 16mm*400mm,t 0.5,1.0,2.0,3.0mm
Dhir et al.[9]	0.1MPa Water	Bottom flooding	1 30 cm/s	-	22,50 •	1127 •	Zircaloy,SUS	Vertical tube t0.71mm(Zircaloy), t 0.88mm (SUS) O.D.0.91cm*1.22m
Iloeje et al.[10]	6 MPa Water	Internal flow	67.8 678 kg/m^2s	-	275 • Saturation	593 •	Inconel X-750	Vertical tube I.D.Φ0.492in.xO.DΦ1in*4in
Chan et al.[11]	0.1MPa Water	Internal two phase flow	35 110 mL/s	-	8,22,45 •	280 600 •	Zircaloy-2	Horizontal tube O.D.Φ19.6mm*2m,t 0.898mm
Okubo et al.[12]	0.1MPa Water	Mist flow	$4.3*10^{-4}$ $4.72*10^{-3}$ $m^3/(m^2s)$	-	21 •	600 100	Argenti SUS304 Silica galass	Vertical cylinder Φ15mm(fixation) Argenti L=1 40mm,SUS L=1.5 7mm Silica L=1.5mm